Bioorganic & Medicinal Chemistry 20 (2012) 6803–6810

Contents lists available at SciVerse ScienceDirect

Bioorganic & Medicinal Chemistry

journal homepage: www.elsevier.com/locate/bmc

Characterization of chlorophyll pigments in the mutant lacking 8-vinyl reductase of green photosynthetic bacterium *Chlorobaculum tepidum*

Tadashi Mizoguchi [a], Jiro Harada [b], Hitoshi Tamiaki [a,*]

[a] *Graduate School of Life Sciences, Ritsumeikan University, Kusatsu, Shiga 525-8577, Japan*
[b] *Depatment of Medical Biochemistry, Kurume University School of Medicine, Kurume, Fukuoka 830-0011, Japan*

ARTICLE INFO

Article history:
Received 10 September 2012
Revised 26 September 2012
Accepted 27 September 2012
Available online 4 October 2012

Keywords:
Chlorophylls
8-Vinyl reductase
Green sulfur bacteria
Photosynthesis

ABSTRACT

The mutant lacking the enzyme BciA (renamed CT1063), which catalyzed reduction of the 8-vinyl group of a porphyrinoid-type 3,8-divinyl-(proto)chlorophyllide-*a* [DV-(P)Chlide-*a*] in the green sulfur bacterium *Chlorobaculum* (*Cba.*) *tepidum*, was reconstructed on the basis of the previous study reported by Chew and Bryant [*J. Biol. Chem.* **2007**, *282*, 2967–2975]. *Cba. tepidum* biosynthesizes the following three different types of chlorophylls (Chls) through their common precursory DV-(P)Chlide-*a* as its photosynthetically active pigments: bacteriochlorophyll(BChl)-*c* and Chl-*a* with the partially reduced 17,18-*trans*-dihydroporphyrin and BChl-*a* with the further reduced 7,8-*trans*-17,18-*trans*-tetrahydroporphyrin. The structures of Chls thus produced were characterized in detail by various spectroscopic techniques. In the mutant, both BChl-*c* and Chl-*a* possessing the alkyl group at the 8-position were exclusively replaced by their 8-vinylated derivatives, whereas BChl-*a* possessed the original 8-ethyl group. The present observations were inconsistent with the previous report. However, it was apparently confirmed that the enzyme BciA was responsible for the reduction of DV-(P)Chlide-*a* to produce BChl-*c* and Chl-*a*. Noteworthily, exclusive accumulation of the reduced (8-ethylated) form of BChl-*a*, not its 8-vinylated derivative, in the mutant indicates the presence of another enzyme catalyzing the 8-vinyl reduction as yet unidentified or any other reduction mechanism using a known enzyme to yield BChl-*a*.

1. Introduction

Chlorophylls (Chls) are one of the most recognized and most abundant types of pigments on the earth.[1] Chl pigments have evolved to fulfill several functions in photosynthesis: they absorb light and transfer it with high efficiency to reaction centers (RCs) where specialized Chls are active in primary charge-separation and energy-transduction processes.[2,3] Chls undergo different modifications during their biosynthesis[4–7] and a variety of Chls are found especially in light-harvesting (LH) complexes not in RCs.[8,9] These chemical modifications help organisms to fine-tune absorption and energy transfer features of the LH complexes.

A major distinction among various classes of Chls which defines characteristic spectral features is the degree of (un)saturation of π-conjugated macrocycles: the fully conjugated porphyrin macrocycle in Chl-*c* of chromophyte algae, chlorin with the 17,18-*trans*-dihydroporphyrin in Chls-*a*/*b*/*d*/*f* of oxygenic organisms and also in bacteriochlorophylls(BChls)-*c*/*d*/*e*/*f* of green anoxygenic bacteria, and bacteriochlorin with the 7,8-*trans*-17,18-*trans*-tetrahydroporphyrin in BChls-*a*/*b*/*g* of anoxygenic bacteria (the latter two types of macrocycles are seen in Fig. 1).[2,9–13]

Chemical modifications of Chls during their biosynthesis have been widely investigated by molecular genetic techniques.[6–8] Most of the enzymes catalyzing the modifications have been identified and mutants lacking a specific enzyme are known. All mature Chls are assumed to be biosynthesized through the common porphyrinoid-type precursor, 3,8-divinyl-(proto)chlorophyllide-*a* [DV-(P)Chlide-*a*] (the structure seen at left in the Graphical Abstract). DV-PChlide-*a* is site-selectively reduced at its 8-vinyl group to afford the mono-vinyl type of PChlide-*a* (=3-vinyl-8-ethyl-PChlide-*a*) by an 8-vinyl reductase.[4,7] PChlide-*a* is further reduced at the C17=C18 moiety by a light-(in)dependent oxidoreductase to the chlorin-type of Chlide-*a*.[14,15] Recently, an alternative pathway has been proposed for the 8-vinyl reduction: the C17=C18 of DV-PChlide-*a* is first reduced to DV-Chlide-*a* and the 8-vinyl group of DV-Chlide-*a* is then reduced to Chlide-*a*.[6,16,17] The remaining reactive 3-vinyl group is further modified to other substituents: 3-CHO in Chl-*d*, 3-$COCH_3$ in BChl-*a* and 3-$CH(OH)CH_3$ in BChls-*c*/*d*/*e*/*f*. Thus, the reduction of the 8-vinyl group of DV-(P)

Abbreviations: APCI, atmospheric pressure chemical ionization; BChl, bacteriochlorophyll; *Cba.*, *Chlorobaculum*; Chl, chlorophyll; DV-(P)Chlide-*a*, 3,8-divinyl-(proto)chlorophyllide-*a*; FMO, Fenna-Matthews-Olson; LH, light-harvesting; NOE, nuclear Overhauser effect; RC, reaction center; ROESY, rotating frame Overhauser enhancement spectroscopy; THF, tetrahydrofuran. .

* Corresponding author. Tel.: +81 77 561 2765; fax: +81 77 561 2659.
E-mail address: tamiaki@fc.ritsumei.ac.jp (H. Tamiaki).

0968-0896/$ - see front matter © 2012 Elsevier Ltd. All rights reserved.
http://dx.doi.org/10.1016/j.bmc.2012.09.054

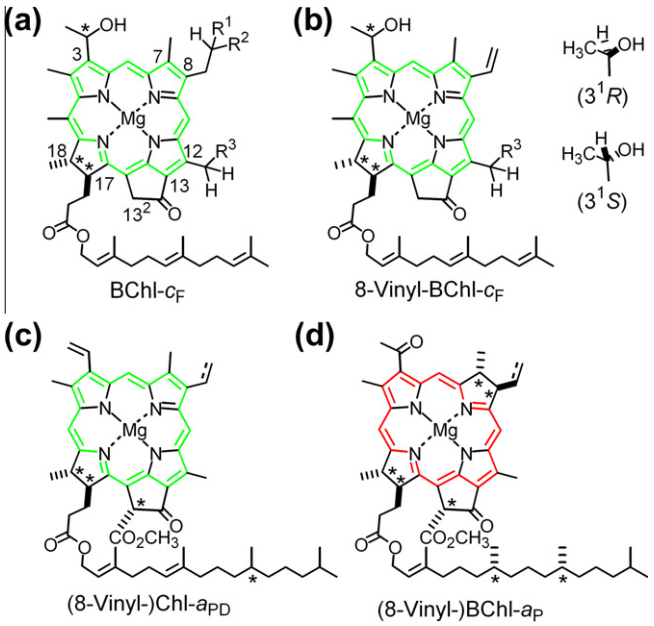

Figure 1. Molecular structures of Chls found in the wild type and its *bciA* mutant of *Cba. tepidum*. Optically active carbon atoms are indicated by asterisks. R^1, R^2 and R^3 (in BChl-*c*) =H or CH_3. The numbering on partial carbon atoms is given by IUPAC-IUB nomenclature.

Chlide-*a* is the key step in producing a variety of Chls in nature, and the content and composition of Chls are important for physiological and taxonomic parameters of photosynthetic organisms.

Green sulfur photosynthetic bacteria biosynthesize three different types of Chls, that is BChl-*c*, Chl-*a* and BChl-*a*, as their photosynthetically active pigments.[18,19] The genome of a green sulfur bacterium *Chlorobaculum* (*Cba.*) *tepidum* contains homologs of two genes, *CT1063* and *CT2014*[20] which have been reported to encode the 8-vinyl reductase of DV-(P)Chlide-*a* in plants (*Arabidopsis thaliana*)[16,17] and purple bacteria (*Rhodobacter capsulatus*),[21] respectively. Both genetic and biochemical analyses showed the gene *CT1063* called *bciA*, not *CT2014* known as *bciB*, encoded the 8-vinyl reductase of DV-PChlide-*a* in *Cba. tepidum*.[22] It was noted that all three types of Chls in the mutant lacking *bciA* of *Cba. tepidum* were replaced by their 8-vinylated derivatives without causing any growth defect for the organism. Here, we reconstructed the mutant lacking the *bciA* and reinvestigated the structures of three types of the resulting Chls in detail to confirm the activity of the enzyme BciA as an 8-vinyl reductase in *Cba. tepidum*.

2. Results and discussion

2.1. Molecular structures of Chls found in *Cba. tepidum* and its mutant lacking 8-vinyl reductase

Green sulfur bacteria including the present *Cba. tepidum* biosynthesize three different types of Chl pigments: BChl-c_F (esterified with farnesol as the 17-propionate), Chl-a_{PD} (with Δ2,6-phaytadienol) and BChl-a_P (with phytol) as shown in Figure 1 (the subscripts 'F', 'PD' and 'P' are abbreviations of hydrocarbon moieties in the 17-propionate), as their photosynthetically active pigments.[9,18,23]

2.1.1. BChl-c_F

BChl-c_F as shown in Figure 1a is present in LH antennae called chlorosomes and is characterized by the presence of a 3-(1-hydroxyethyl) group, a central magnesium and a 13-carbonyl group and by the lack of a 13^2-methoxycarbonyl group in a molecule. These functional groups are aligned to the y axis of a molecule. Based on such structural features, BChl-*c* spontaneously forms well-ordered self-aggregates through the coordination and hydrogen bonds: Mg ••• O(3^2)–H ••• O=C(13^1).[23–25] The aggregates constitute the core part of chlorosomes and play the key role in harvesting light-energy and transferring it to photochemical RCs via energy-accepting apparatuses [baseplate and Fenna-Matthews-Olson (FMO) proteins] composed of BChl-*a* (*vide infra*). BChl-*c* is a mixture of diastereomers at the chiral 3^1-position as well as homologs with different degrees of methylation at the 8^2- and 12^1-positions. The (3^1*R*)-epimers having an ethyl (E), propyl (P) or isobutyl (I) group at the 8-position and a methyl (M) or ethyl group at the 12-position are termed R[E,M], R[E,E], R[P,E] and R[I,E]. The (3^1*S*)-epimers are termed similarly, S[E,E], S[P,E] and S[I,E]. In green sulfur bacteria, BChls-*c* are mainly esterified with C15 farnesol as their 17-propionate residues instead of the usual C20 phytol found in most naturally occurring Chls, although several different long chains as the 17-propionate residue have also accumulated as minor components.

2.1.2. Chl-a_{PD}

Chl-a_{PD} as shown in Figure 1c is an analog of the best known and most abundant Chl pigment, Chl-a_P, on the earth. The structural difference between the two types of Chl-*a* is only in their 17-propionates: phytol for Chl-a_P and Δ2,6-phytadienol for Chl-a_{PD}. Chl-a_{PD} is present in the photosystem I-type of RCs of green sulfur bacteria and functions as the primary electron acceptor in the RCs.[19,26]

2.1.3. BChl-a_P

BChl-*a* with a bacteriochlorin π-skeleton (7,8-reduced form of chlorin moiety in the above mentioned BChl-*c* and Chl-*a*) as shown in Fig. 1d acts as the first and the second acceptor (baseplate and FMO proteins, respectively) of light energy from the core LH part of chlorosomes and is also photosynthetically active pigments in RCs.[18,23]

2.1.4. BChl-c_F, Chl-a_{PD} and BChl-a_P in the mutant lacking 8-vinyl reductase

During the biosynthesis of all three Chls mentioned above, the 8-vinyl group in their common precursory DV-PChlide-*a* was reported to be reduced to an ethyl group by the enzyme BciA.[5,22] In the case of BChl-c_F, the ethyl group was further methylated once or twice by the enzyme BchQ (for the methylation at the 8^2-position) and similarly the 12-methyl group was methylated by BchR to form various homologs as seen in Figure 1a.[27] It was previously reported that the mutant lacking *bciA* of *Cba. tepidum* accumulated 8-vinyl derivatives of all three Chls as shown in Figure 1b–d.[22] To evaluate the activity of the BciA enzyme, we reconstructed the *bciA* mutant of *Cba. tepidum* on the basis of the reported method[22] (see Fig. S1A), and reinvestigated the structural changes of the three Chls following the mutation.

2.2. Three types of Chls found in *Cba. tepidum*

Figure 2a shows the normal-phase HPLC profile of the extract containing three types of Chls from the cells of the *bciA* mutant of *Cba. tepidum*, according to the method of Kobayashi et al. (data on the wild type are cited in Fig. S2).[19] The relative content of the three Chls was estimated to be BChl-c_F/Chl-a_{PD}/BChl-a_P = 96.7:0.2:3.1 from the peak areas of HPLC (the ratio for the wild type of 96.4:0.3:3.3). Details of the estimation are ascribed in Fig. S2. To confirm the minor Chl-a_{PD} and BChl-a_P in the profile, mass chromatograms (m/z = 889.5 and 911.5) were applied as shown in Figure 2b and c. Based on the mass chromatograms,

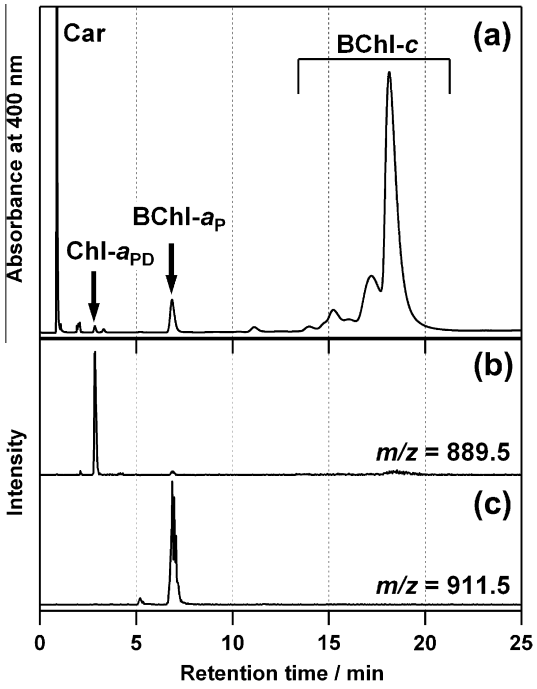

Figure 2. Normal-phase HPLC profile detected at 400-nm absorbance (a) and selective mass chromatograms at m/z = 889.5 for Chl-a_{PD} (b) and 911.5 for BChl-a_P (c) of the extract containing three types of Chls from the cells of the *bciA* mutant of *Cba. tepidum*. HPLC conditions: Column, Cosmosil 5SL-II (3.0 × 150 mm); eluent, hexane/2-propanol/methanol = 100:1.5:0.2 (v/v/v); flow rate, 1.0 mL/min. Car indicates carotenoid.

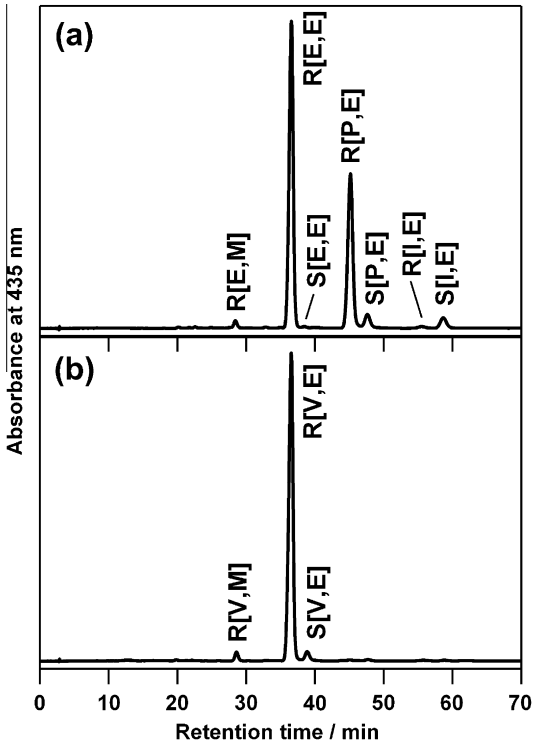

Figure 3. Representative reverse-phase HPLC profiles of BChl-c_F extracts from the cells of the wild type (a) and the *bciA* mutant (b) of *Cba. tepidum*. The cells were harvested at the stationary phase of the cultivation. HPLC conditions: Column, Cosmosil 5C18-AR-II (4.6 × 250 mm), eluent, acetonitrile/acetone/H_2O = 65:15:20 (v/v/v); flow rate, 1.0 mL/min.

Chl-a_{PD} (exact mass, 888.50) and BChl-a_P (910.55) were identified as their protonated forms ($[MH]^+$) at the retention times of 2.9 and 6.9 min, respectively. Each on-line absorption spectrum also supported the assignment (Fig. S2d as an example). Chl-a_{PD} and BChl-a_P were thus fractionated by the HPLC and are further characterized in Section 2.3.3. Since separation of an epimeric and homologous mixture of BChl-*c* eluted at the retention times of 13–21 min was not sufficient for characterization under these HPLC conditions, detailed analysis of a mixture of BChl-c_F was done in the next Section, 2.3.1, using high-resolution reverse-phase HPLC.

2.3. Characterization of Chls found in *Cba. tepidum* and its mutant lacking 8-vinyl reductase

2.3.1. A variety of BChl-*c* epimers and homologs in LH chlorosomes

Figure 3a shows a representative reverse-phase HPLC profile monitored at 435 nm for the extracts from the cells of the wild type of *Cba. tepidum*. Several BChl-*c* components were detected as the pigments absorbing a 435-nm light. According to previous reports on the accumulation of several BChl-*c* molecules in *Cba. tepidum*,[28,29] these seven peaks were safely assigned to BChls-*c* having different degrees of the methylation at the 8^2- and 12^1-positions as well as stereochemistry at the chiral 3^1-position: R[E,M], R[E,E], S[E,E], R[P,E], S[P,E], R[I,E] and S[I,E] forms of BChl-c_F in the order of elution (see the abbreviations in Section 2.1). The assignment was confirmed by on-line LCMS as shown in Table 1 and by the ^{1}H NMR spectrum for the dominant R[E,E]BChl-c_F in Fig. S3b (see details in Section 2.3.2).

The pigment composition of the *bciA* mutant was quite different from that of the wild type as shown in Figure 3. In the *bciA* mutant, the homologs with methylation at the 8^2-position were completely eliminated due to the absence of a characteristic ethyl group at that position. A predominant pigment at the retention time of 36.5 min was observed. The pigment exhibited a red-shifted Soret absorption at 440.6 nm and almost no shift of the Qy absorption at 660.2 nm in Et_2O in comparison with R[E,E]BChl-c_F (432.4 and 660.6 nm) from the wild type as shown in Figure 4a, and was assumed to the 8-vinyl form of BChl-*c*. Chl pigments having an 8-vinyl group generally showed their red-shifted Soret absorption and almost no shift of the Qy absorption, compared with the corresponding 8-ethylated analog: Chl-a_P (429.6/660.8 nm in Et_2O) and 8-vinyl-Chl-a_P (436.2/659.8 nm in Et_2O) as examples.[22,30] The relative content of the dominant R[V,E]BChl-c_F was estimated to be 94.7% of the total BChl-c_F in the mutant by the peak areas of HPLC.

Table 1
APCI-mass spectrometric data of BChls-*c* from full-grown cells of *Cba. tepidum* and its *bciA* mutant

Pigment species (retention time/min)	Observed peaks			Calculated for	
	Molecular-ion[a]	Fragment 1[b]	Fragment 2[c]	$[MH]^+$	Fragment 1
R[E,M]BChl-*c* (28.4)	793.5	589.1	775.3	793.45	589.26
R[E,E]BChl-*c* (36.6)	807.4	603.2	789.4	807.46	603.27
S[E,E]BChl-*c* (38.4)	807.3	—[d]	789.3	807.46	603.27
R[P,E]BChl-*c* (45.1)	821.4	617.2	803.4	821.48	617.29
S[P,E]BChl-*c* (47.6)	821.4	617.3	803.4	821.48	617.29
R[I,E]BChl-*c* (55.5)	835.4	—[d]	817.4	835.49	631.31
S[I,E]BChl-*c* (58.6)	835.4	631.3	817.4	835.49	631.31
R[V,M]BChl-*c* (28.6)	791.3	587.2	773.4	791.43	587.24
R[V,E]BChl-*c* (36.5)	805.3	601.2	787.3	805.45	601.26
S[V,E]BChl-*c* (38.9)	805.3	601.1	787.4	805.45	601.26

[a] $[MH]^+$.
[b] Protonated bacteriochlorophyllide-*c* ($[M-farnesyl+2H]^+$).
[c] $[M-OH]^+$ or $[M-H_2O+H]+$.
[d] Not identified.

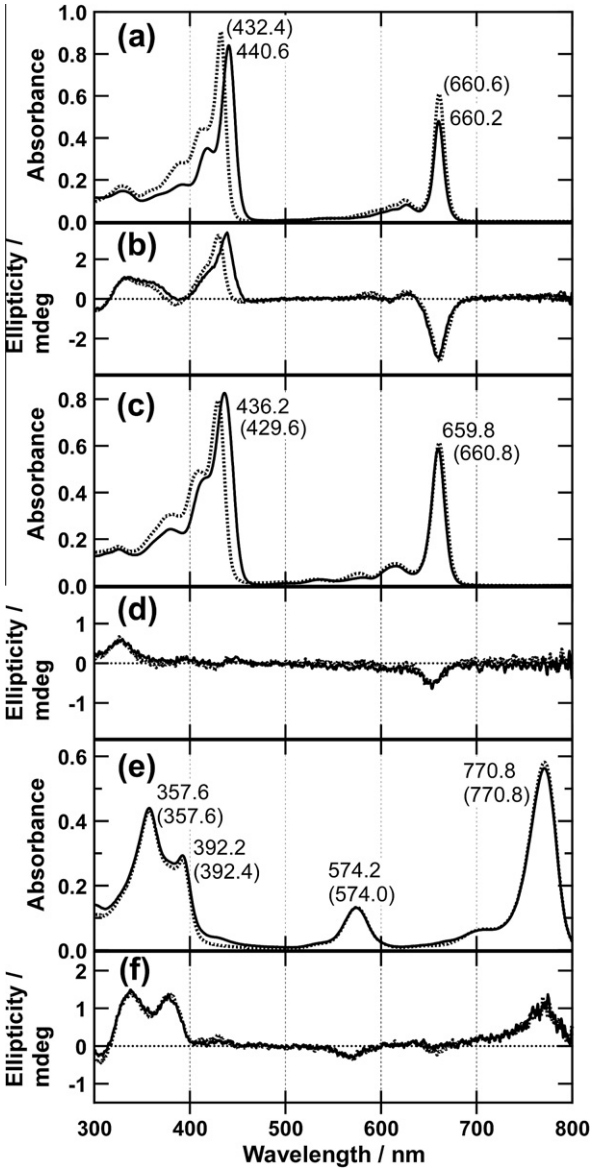

Figure 4. UV–vis (a,c,e) and CD spectra (b,d,f) of the isolated Chls in Et_2O: (a,b) R[E,E]BChl-c_F from the wild type (dotted) and R[V,E]BChl-c_F from the *bciA* mutant (solid) of *Cba. tepidum*; (c,d) Chl-a_{PD} from the wild type (dotted) and 8-vinyl-Chl-a_{PD} from the mutant (solid); (e,f) BChl-a_P from the wild type (dotted) and the mutant (solid). Absorption maxima of each pigment from the mutant are labeled: the values from the wild type shown in parenthesis.

The content was almost independent upon bacterial cultivation (see Table S1 on the composition of BChls-c_F at different growth stages).

2.3.2. Structural determination of R[V,E]BChl-c_F in the *bciA* mutant

From electronic-absorption properties of BChl-*c* synthesized in the *bciA* mutant as shown in Figure 4a, we expected the newly accumulated pigments to be the 8-vinylated derivative of BChl-*c*.

R[V,E]BChl-c_F, a major homolog of BChl-*c* in the mutant, was fully characterized by its ^{1}H NMR and mass spectra. The pigment gave the molecular-ion peak at $m/z = 805.3$ (see Table 1 and Fig. S4), which was consistent with the value of the protonated pigment (calcd for 805.45). One of the fragment peaks (fragment 1 in Table 1 and Fig. S4) was observed at $m/z = 601.2$ produced by the loss of the esterifying group in the 17-propionate residue, indicating that the pigment had a C15 farnesyl group: 805.3−601.2 = 204.1 = $C_{15}H_{25}$−H. Moreover, another fragment peak was observed at $m/z = 787.3$ due to the loss of 17 in mass number (fragment 2 in Table 1 and Fig. S4), supporting the presence of a hydroxy group in a molecule.

Figure S3 shows a representative 1D-^{1}H NMR spectrum of the purified R[V,E]BChl-c_F in tetrahydrofuran (THF)-d_8 at room temperature, together with the corresponding 8-ethylated R[E,E]BChl-c_F isolated from the cells of the wild type. We can clearly find the presence of the proton signals originating from the characteristic vinyl group in R[V,E]BChl-c_F (chemical shifts, $\delta_H = 8.18$, 6.17 and 5.87 ppm) and the lack of the signals from 8-CH_2CH_3 found in R[E,E]BChl-c_F (3.80 and 1.71 ppm). In order to determine the molecular structure, especially for location of the vinyl group, we employed 2D-NMR spectroscopy. The inset of Figure S3 summarizes the observed nuclear Overhauser effect (NOE) correlations in the rotating frame Overhauser enhancement spectroscopy (ROESY) spectrum using arrows. These NOE correlations established the molecular structure of R[V,E]BChl-c_F, starting from the 5-*meso* proton the signal was definitely assigned. The evidence obtained from NMR and mass measurements was fully consistent with the molecular formulation shown in Figure 1b.

Remaining undetermined structures were the stereochemistry at the chiral 3^1-, 17- and 18-positions (see Fig. 1b). To confirm the 3^1-configuration, R[V,E]BChl-c_F was modified to R[E,E]BChl-c_F by hydrogenation with rhodium catalyst on alumina[31] of the 8-vinyl group in R[V,E]BChl-c_F to an ethyl group as shown in Fig. S5a. The resultant hydrogenated R[E,E]BChl-c_F was analyzed by co-chromatography with naturally occurring R[E,E]BChl-c_F isolated from the wild type. It showed the identical elution time on HPLC as in Figure S5b. Since a pair of stereoisomers at the 3^1-position of BChl-*c* could be separated by conventional HPLC as depicted in Figure 3a, the stereochemistry at the chiral 3^1-position of the major [V,E]BChl-c_F was confirmed to be (3^1R)-configuration.

To confirm the configurations at the chiral 17- and 18-positions, we used NOE correlations and CD spectra. The *syn*-orientations of 17-CH_2CH_2 and 18-H (17-H and 18-CH_3) were confirmed based on the NOE correlations as shown in the inset molecular structure of Fig. S3: 17-H ↔ 18-CH_3, 17^1-H_2 ↔ 18-H and 17^2-H_2 ↔ 18-H. From these NOE correlations, the stereochemistry was established to be 17-(*S*)- and 18-(*S*)-configurations or its mirror image 17-(*R*)- and 18-(*R*)-configurations. To distinguish the pair of enantiomers confirmed above, we used CD spectroscopy. Figures 4b and S5d show the CD spectra of natural R[E,E]BChl-c_F and R[V,E]BChl-c_F as well as synthetic R[E,E]BChl-c_F in Et_2O (or THF). All the pigments exhibited negative and positive CD signals at the Qy and Soret regions, respectively. The results indicate that they have the same stereochemistry at the chlorin chromophore, so the absolute configurations at the 17- and 18-positions of R[V,E]BChl-c_F were characterized to be 17-(*S*)- and 18-(*S*)-configurations generally seen in Chl pigments. By comparison of retention times of BChls-*c* in the wild type and the mutant of *Cba. tepidum* as well as on-line LCMS data in Table 1, the other minor homologs were assigned to R[V,M]BChl-c_F (at the retention time of 28.6 min) and S[V,E]BChl-c_F (at 38.9 min). Thus, all BChls-*c* in the mutant lacking *bciA* carried the vinyl group at the 8-position, and the enzyme BciA was responsible for reduction of the 8-vinyl group to yield BChl-*c* as reported by Chew and Bryant.[22]

2.3.3. Structural characterization of 8-vinyl-Chl-a_{PD} in the *bciA* mutant

Figure 4c shows the electronic-absorption spectra of Chl-a_{PD} isolated from the wild type (dotted) and the *bciA* mutant (solid) of *Cba. tepidum*. A red-shift of the Soret absorption maxima (429.6 to 436.2 nm) and a slight blue shift of the Qy absorption maxima (660.8 to 659.8 nm) by the mutation were observed

similar to those found in BChl-*c* (see also Fig. 4a). These absorption changes strongly indicated substitution of an ethyl group with a vinyl group at the 8-position. The two Chl-a_{PD} species were further characterized by HPLC as shown in Figure 5a. The two Chl-a_{PD} pigments showed different retention times: 38.5 min for the mutant and 40.1 min for the wild type. In on-line mass spectra of Figure 5b, a 2.0 Da mass difference was given and the species from the mutant gave another molecular-ion peak by a 2.0 mass number smaller than that from the wild type. Fragmented-ion peaks showed the Δ2,6-phytadienyl ester in the two Chls-*a* (see Section 3.3). Moreover, the two Chl-a_{PD} gave identical CD signs as shown in Figure 4d, indicating identical stereochemistry at the 13^2-, 17- and 18-positions, (13^2R)-, (17*S*)- and (18*S*)-configurations. The results confirmed that the mutant produced 8-vinyl-Chl-a_{PD} and the enzyme BciA was responsible for reduction of the 8-vinyl group to yield Chl-a_{PD} as reported by Chew and Bryant.[22]

2.3.4. Structural identification of BChl-a_P in the *bciA* mutant

Figure 4e and f show the electronic-absorption and CD spectra, respectively, of the BChl-a_P species isolated from the wild type (dotted) and the *bciA* mutant (solid). No shift of the Soret absorption was observed, which is inconsistent with the absorption spectral changes in BChl-*c* and Chl-a_{PD} as mentioned above. Figure 5c shows co-chromatographic analysis of an equimolar mixture of the two BChl-*a* isolated from the wild type and the *bciA* mutant to give a single peak at 27.2 min. The peak afforded a mass spectrum identical to the original BChl-a_P from the wild type. Based on the results, the two BChl-a_P species isolated from the wild type and the *bciA* mutant were concluded to be identical. No molecular-ion peak originating from 8-vinyl-BChl-a_P (2.0 Da mass smaller than 8-ethylated BChl-a_P) was observed as seen in Figure 5d, indicating that reduction of the 8-vinyl group in BChl-*a* further continued to proceed during the biosynthesis even in the absence of BciA. It is noteworthy that the enzyme BciA is not always involved in the reduction of the 8-vinyl group to yield BChl-a_P and that another enzyme catalyzing the reduction is present or that some other reduction mechanism in *Cba. tepidum* operates. This observation was inconsistent with the previous report that 8-vinyl-BChl-a_P was produced in the mutant.[22] The contradiction is probably ascribed to the HPLC methods for analyses of three different types of Chls in *Cba. tepidum*: each isolated Chl analyzed by isocratic HPLC in the present study and a mixture of three Chls by binary-gradient HPLC in the previous report. The precise analysis of BChl-*a* seems to be difficult in the latter HPLC, since hydrophobicity of the Chls is quite different. Additionally, the presence of a trace degradation product of BChl-*a* during the analysis should be noted. BChl-*a* easily produces its C7−C8 oxidized derivative, 3-acetyl-Chl-a_P, which has the identical mass number to 8-vinyl-BChl-a_P.

2.4. Reduction of the 8-vinyl group in green sulfur bacteria

As the mutant lacking *bciA* exclusively accumulated the 8-vinyl forms of BChl-*c* and Chl-a_{PD} as well as the reduced (8-ethyl) form of BChl-*a*, we investigated photosynthetic activity of the *bciA* mutant by several spectroscopic measurements.

Figure 6a shows electronic-absorption spectra of the cells of the wild type (dotted) and its *bciA* mutant (solid). The intense

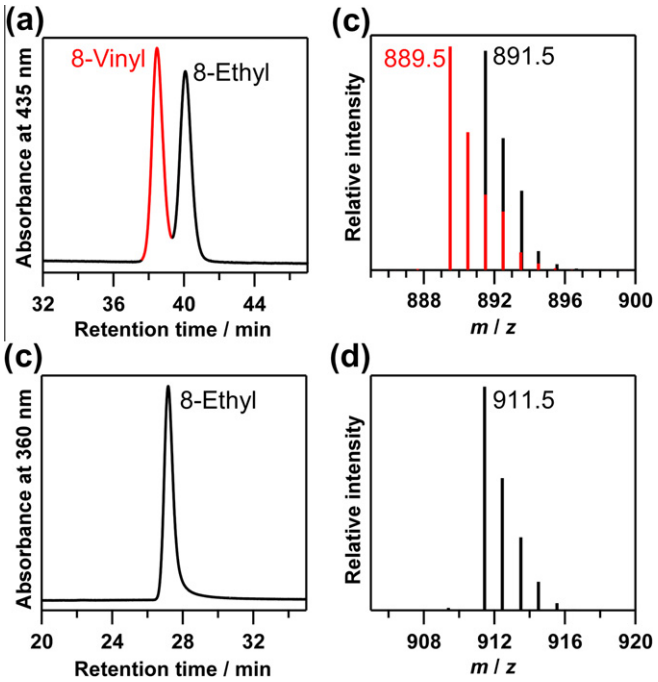

Figure 5. Co-chromatographic HPLC (a,c) and APCI-MS analyses (b,d) of the two Chl-a_{PD} (a,b) and BChl-a_P species (c,d) isolated from the wild type and the *bciA* mutant of *Cba. tepidum*. HPLC conditions: (a), Cosmosil 5SL-II (6.0 × 250 mm), hexane/2-propanol/methanol = 100:0.7:0.1 (v/v/v), 1.0 mL/min, (c), Cosmosil 5SL-II (6.0 × 250 mm), hexane/2-propanol/methanol = 100:1.5:0.2 (v/v/v), 1.0 mL/min. In (b), MS spectra at 38.5 and 40.1 min are shown in red and black, respectively.

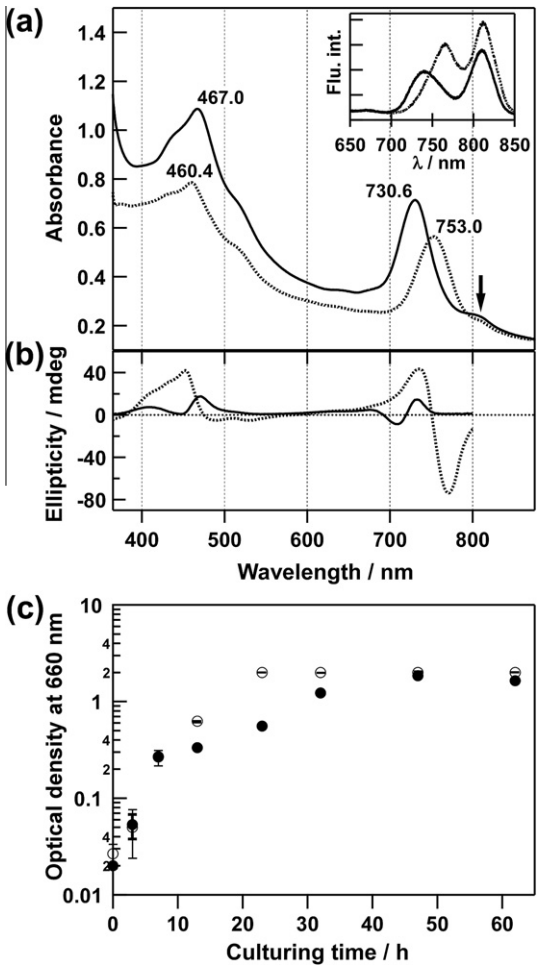

Figure 6. Electronic-absorption and fluorescence-emission (a) and CD spectra (b) of the cells of the wild type (dotted) and the *bciA* mutant (solid) of *Cba. tepidum* in 50 mM Tris–HCl buffer (pH 8.0) containing 20 mM $Na_2S_2O_4$, and growth profiles (c) of the wild type (open circles) and the mutant monitored at 660 nm (closed circles). The fluorescence-emission spectra were obtained by excitation at the Soret absorption maxima.

absorption bands were ascribable to the self-aggregates of BChl-*c* in LH chlorosomes. The difference in the Qy maxima (730.6 nm for the mutant and 753.0 nm for the wild type) is mostly ascribable to the composition of BChl-*c* species. BChl-*c* in the wild type was composed of a mixture of various homologs with different methylation at the 8^2- and 12^1-positions, while in the mutant such a variety was almost completely eliminated by substitution of the vinyl group at the 8-position as shown in Figure 3. This is consistent with the previous reports on the mutant lacking the enzymes BchQ and BchR catalyzing methylation at the 8^2- and 12^1-positions, respectively, of *Cba. tepidum*.[27]

The bands at ~805 nm observed in both the wild type and the *bciA* mutant as indicated by the arrow in Figure 6a are ascribable to BChl-*a* molecules in chlorosomal baseplate, FMO proteins and/or RCs. The inset panel of this figure shows the fluorescence-emission spectra of the cells excited at the Soret absorption maxima of BChl-*c* self-aggregates. Upon the excitation, efficient energy transfer to BChl-*a* molecules was observed in both the wild type and the *bciA* mutant. Thus, the 8-vinylated BChl-*c* functioned as the photosynthetically active pigment in the *bciA* mutant, although the energy gap between energy donating BChl-*c* self-aggregates and energy accepting BChl-*a* in the mutant was larger than that in the wild type: the gaps in absorption maxima were calculated to be about 1300 cm^{-1} and 900 cm^{-1} for the mutant and the wild type, respectively. The substitution of the 8-vinyl group in some alkyl groups also affected the supramolecular structure of the self-aggregates. This was confirmed by most CD signs being reversed as shown in Figure 6b, especially for the Qy bands of the *J*-type aggregates of BChl-*c*.

Figure 6c shows growth profiles of the wild type (open circles) and its *bciA* mutant (closed circles). The *bciA* mutant could grow using the 8-vinyl forms of BChl-*c* and Chl-a_{PD} as well as the 8-ethyl form of BChl-*a* as the photosynthetically active pigments, although the growth rate of the mutant was slightly slower than that of the wild type: the growth rates (doubling times) were calculated to be 0.074 ± 0.002 h^{-1} (9.3 ± 0.3 h) for the mutant and 0.139 ± 0.002 h^{-1} (5.1 ± 0.1 h) for the wild type. This is probably due to the larger energy gap between BChl-*c* self-aggregates and BChl-*a* in the mutant. Therefore, the alkylated (not vinyl) form of BChl-*c* might be crucial for efficient photosynthetic activity of *Cba. tepidum*.

3. Experimental

3.1. Bacterial strains and culture conditions

The strain WT2321 of *Cba. tepidum*[32] was used as the wild type and host for transformation. This strain was anaerobically grown in screw-capped bottles with liquid CL media or on solid CP plates[33] at 40 or 45 °C. *Escherichia coli* DH5α was grown in LB medium containing 100 μg/mL of ampicillin or 10 μg/mL gentamycin.

3.2. Plasmid constructions and natural transformation of *Cba. tepidum*

The PCR primers used in this study for the construction of plasmids are described in Table S2. To construct the *Cba. tepidum* mutant lacking *bciA* gene, the plasmid pTA2-tepbciAGm was produced as follows. A 1.91 kbp DNA fragment containing the *bciA* gene was amplified from genomic DNA by PCR using primers BCIA F1 and R1. The product was ligated into the TA-cloning site of T-Vector pTA2 (TOYOBO, Osaka, Japan) according to the manufacturer's protocol, yielding pTA2-tepbciA plasmid. The *aacC1* gene, conferring resistance to gentamycin, was excised from pUCGM[34] using *Sma*I. The pTA2-tepbciA was used as template for PCR using DNA polymerase KOD-plus-(TOYOBO) with primer set BCIA F2 and R2. The resulting PCR product was ligated to the *aacC1* gene, creating pTA2-tepbciAGm plasmid.

Natural transformation of *Cba. tepidum* with the pTA2-tepbciAGm to construct a *bciA* lacking mutant was performed as previously described.[33,35] After obtaining transformants, PCR analysis was carried out to check segregation of the wild type and mutant alleles using primers Tep.bciA comf. F and R. The product amplified from the genomic DNA of the *bciA* mutant was digested with *Eco*RV, and then analyzed by agarose gel electrophoresis using a DNA molecular weight marker, λ/*Sty*I digest (TOYOBO), to estimate the molecular mass of the DNA fragments (Fig. S1B).

3.3. Determination and isolation of Chl-a_{PD} and BChl-a_P

Pigments of the wild type and its *bciA* mutant of *Cba. tepidum* were extracted and analyzed as follows. A mixture of acetone and methanol (9/1, v/v) was added to the harvested cells and mixed using a vibrator. A mixture of diethyl ether and petroleum ether (1/1, v/v) and then distilled water were added to transfer the pigment components to the ether layer. The ether phase was collected and evaporated to dryness by a stream of N_2 gas, and the residues were dissolved in a small amount of the following HPLC eluent. The LCMS analysis was performed using a Shimadzu LCMS-2010EV system (Shimadzu, Kyoto, Japan) comprising a liquid chromatograph (an SCL-10Avp system controller, an LC-10ADvp pump, and an SPD-M10Avp photodiode-array detector) and a quadrupole mass spectrometer equipped with an atmospheric pressure chemical ionization (APCI) probe. Normal-phase HPLC was performed under the following conditions: column, Cosmosil 5SL-II (3.0 × 150 mm for analysis, 4.6 × 150 mm for preparation, Nacalai Tesque, Kyoto); eluent, hexane/2-propanol/methanol = 100:1.5:0.2 (v/v/v) for analysis, hexane/THF = 82.5:17.5 (v/v) for preparation; flow rate 1.0 mL/min for both analysis and preparation. APCI-MS spectra were measured as follows: resolution, ±0.15 Da; capillary temperature, 250 °C; APCI vaporizer temperature, 400 °C; ionization voltage, 4.5 kV; sheath gas flow, 2.5 L/min; drying gas pressure, 0.02 MPa.

3.3.1. BChl-a_P

VIS (Et_2O) λ_{max}/nm 770.8 (relative absorbance, 1.00), 574.2 (0.23), 392.2 (0.52), 357.6 nm (0.78); MS (APCI) found: *m*/*z* 911.6 and 663.2, calcd for $C_{55}H_{74}N_4O_6Mg$: 911.55 ($[MH]^+$) and $C_{35}H_{36}N_4O_6Mg$: 633.25 ($[M-phytyl+2H]^+$).

3.3.2. Chl-a_{PD}

VIS (Et_2O) λ_{max}/nm 660.8 (relative absorbance, 0.77), 616.2 (0.12), 429.6 nm (1.00); MS (APCI) found: *m*/*z* 891.5 and 615.2, calcd for $C_{55}H_{70}N_4O_5Mg$: 891.52 ($[MH]^+$) and $C_{35}H_{34}N_4O_5Mg$: 615.24 ($[M-\Delta2,6\text{-phytadienyl}+2H]^+$).

3.3.3. 8-Vinyl-Chl-a_{PD}

VIS (Et_2O) λ_{max}/nm 659.8 (relative absorbance, 0.71), 615.6 (0.10), 436.2 nm (1.00); MS (APCI) found: *m*/*z* 889.5 and 613.2, calcd for $C_{55}H_{68}N_4O_5Mg$: 889.50 ($[MH]^+$) and $C_{35}H_{32}N_4O_5Mg$: 613.22 ($[M-\Delta2,6\text{-phytadienyl}+2H]^+$).

3.4. Determination of compositions of BChl-*c* homologs

The pigment components were extracted from the harvested cells of the wild type and the *bciA* mutant as mentioned above. The LCMS analysis was also performed as mentioned above, except for HPLC conditions. Reverse-phase HPLC was performed under the following conditions: column, Cosmosil 5C18-AR-II (4.6 × 250 mm, Nacalai Tesque); eluent, acetonitrile/acetone/H_2O = 65:15:20 (v/v/v); flow rate 1.0 mL/min.

3.5. Isolation and structural determination of R[V,E]BChl-c_F

The pigment mixture was extracted from the harvested cells of the wild type and the *bciA* mutant strain as mentioned above. Both R[V,E]BChl-c_F and R[E,E]BChl-c_F, the dominant BChl-c_F in the *bciA* mutant and the wild type, respectively, were purified by the following HPLC: column, Cosmosil 5C18-AR-II (10 × 250 mm, Nacalai Tesque); eluent, methanol/H_2O = 95:5 (v/v); flow rate 1.5 mL/min. The 600 MHz ^{1}H NMR spectra of the isolated R[V,E]BChl-c_F and R[E,E]BChl-c_F were recorded in THF-d_8 (Euriso-top, Saclay, France) using a JEOL ECA-600 NMR spectrometer (JEOL, Akishima, Japan); the residual proton at the 3-position of THF-d_7 (δ_H = 1.72 ppm) was used as an internal standard. A set of assignments of ^{1}H signals was obtained by correlation spectroscopy and ROESY spectra (τ_m = 400 msec).

3.5.1. R[V,E]BChl-c_F

VIS (Et_2O) λ_{max}/nm 660.2 (relative absorbance, 0.57), 627.0 (0.10) and 440.6 nm (1.00); δ_H/ppm 10.01 (1H, s, 5-H), 9.72 (1H, s, 10-H), 8.18 (1H, dd, J = 11.4, 18.0 Hz, 8^1-H), 6.34 (1H, q, J = 6.6 Hz, 3^1-H), 6.17 (1H, d, J = 18.0 Hz, 8^2-H *trans* to C8^1−H), 5.87 (1H, d, J = 11.4 Hz, 8^2-H *cis* to C8^1−H), 5.21 (1H, t, J = 7.1 Hz, f2-H), 5.13, 5.07 (each 1H, d, J = 19.2 Hz, 13^2-H_2), 5.04 (2H, t, J = 6.8 Hz, f6-H, f10-H), 4.95 (1H, d, J = 2.4 Hz, 3^1-OH), 4.71 (2H, q, J = 7.2 Hz, 18-H), 4.49 (2H, m, f1-H_2), 4.21 (1H, m, 17-H), 4.06 (2H, q, J = 7.2 Hz, 12^1-H_2), 3.91 (3H, s, 20-CH_3), 3.45 (3H, s, 7-CH_3), 3.39 (3H, s, 2-CH_3), 2.45 (2H, m, 17^2-H_2), 2.18 (2H, m, 17^1-H_2), 2.02 (each 2H, m, f5-H_2, f9-H_2), 1.98 (3H, d, J = 6.6 Hz, 3^1-CH_3), 1.95 (3H, t, J = 7.2 Hz, 12^1-CH_3), 1.92 (each 2H, m, f4-H_2, f8-H_2), 1.622 (3H, s, f3-CH_3), 1.616 (3H, s, f12-H_3), 1.55, 1.52 (each 3H, s, f7-CH_3, f11-CH_3), 1.54 (3H, d, J = 7.2 Hz, 18-CH_3); MS (APCI) found: m/z 805.3, 787.3 and 601.2, calcd for $C_{50}H_{60}N_4O_4Mg$: 805.45 ([MH]$^+$), $C_{50}H_{59}N_4O_3Mg$: 787.33 ([M−OH]$^+$ or [M−H_2O+H]$^+$) and $C_{35}H_{36}N_4O_4Mg$: 601.26 ([M−farnesyl+2H]$^+$).

3.5.2. R[E,E]BChl-c_F

VIS (Et_2O) λ_{max}/nm 660.6 (relative absorbance, 0.67), 625.0 (0.12) and 432.4 nm (1.00); δ_H/ppm 9.89 (1H, s, 5-H), 9.56 (1H, s, 10-H), 6.34 (1H, q, J = 6.6 Hz, 3^1-H), 5.21 (1H, t, J = 7.2 Hz, f2-H), 5.13, 5.07 (each 1H, d, J = 19.0 Hz, 13^2-H_2), 5.04 (2H, t, J = 7.2 Hz, f6-H, f10-H), 4.89 (1H, d, J = 1.8 Hz, 3^1-OH), 4.70 (1H, q, J = 7.2 Hz, 18-H), 4.48 (2H, m, f1-H_2), 4.21 (1H, m, 17-H), 4.06 (2H, q, J = 7.8 Hz, 12^1-H_2), 3.91 (3H, s, 20-CH_3), 3.80 (2H, q, J = 7.8 Hz, 8^1-H_2), 3.39 (3H, s, 2-CH_3), 3.30 (3H, s, 7-CH_3), 2.46 (2H, m, 17^2-H_2), 2.18 (2H, m, 17^1-H_2), 2.02 (each 2H, m, f5-H_2, f9-H_2), 1.97 (3H, d, J = 6.6 Hz, 3^1-CH_3), 1.95 (3H, t, J = 7.8 Hz, 12^1-CH_3), 1.93 (each 2H, m, f4-H_2, f8-H_2), 1.71 (3H, t, J = 7.8 Hz, 8^1-CH_3), 1.62 (each 3H, s, f3-CH_3, f12-H_3), 1.53 (3H, d, J = 7.2 Hz, 18-CH_3), 1.55, 1.52 (each 3H, s, f7-CH_3, f11-CH_3); MS (APCI) found: m/z 807.5, 789.5 and 603.3, calcd for $C_{50}H_{62}N_4O_4Mg$: 807.46 ([MH]$^+$), $C_{50}H_{61}N_4O_3Mg$: 795.34 ([M−OH]$^+$ or [M−H_2O+H]$^+$) and $C_{35}H_{38}N_4O_4Mg$: 603.27 ([M−farnesyl+2H]$^+$).

3.6. Spectroscopic measurements of bacterial cells and pigments

Electronic-absorption spectra were measured with a Hitachi U-3500 (Hitachi High-Tech, Tokyo, Japan). Fluorescence-emission spectra were measured with a C9920-03G series fluorescence measurement system (Hamamatsu Photonics, Shizuoka, Japan). CD spectra were measured with a Jasco J-720 W spectropolarimeter (Jasco, Tokyo). Cells of the wild type and the *bciA* mutant grown in the early stationary phase under irradiation at about 30 μE s^{-1} m^{-2} were collected, suspended in 50 mM Tris–HCl (pH 8.0), and used for the measurements of electronic-absorption and CD spectra. For the measurements of fluorescence-emission spectra, the cell suspension was mixed with 20 mM sodium dithionite and incubated for 30 min.

3.7. Growth rate measurements of bacteria

Pre-cultures of the wild type and *bciA* mutant of *Cba. tepidum* were grown to stationary phase under irradiation at about 30 μE s^{-1} m^{-2}. Three hundred μL aliquots of pre-cultures were inoculated into 30 mL screw-capped test tubes filled with freshly prepared CL media, and cultures were then grown under illumination of 30 μE s^{-1} m^{-2} at 45 °C. Optical cell densities were measured at 660 nm using a Mini Photo 518R photometer (TAITEC, Saitama, Japan).

Acknowledgements

We would like to thank Dr. T. Yoshitomi and Mr. T. Yajima of Ritsumeikan University for their experimental assistance. This work was partially supported by Grants-in-Aid for Scientific Research (A) (No. 22245030) (to H.T.) and (C) (No. 24550065) (to T.M.) as well as for Young Scientists (B) (No. 24750169) (to J.H.) from the Japanese Society for the Promotion of Science (JSPS).

Supplementary data

Supplementary data associated with this article can be found, in the online version, at http://dx.doi.org/10.1016/j.bmc.2012.09.054.

References and notes

1. Kräutler, B. *Photochem. Photobiol. Sci.* **2008**, *7*, 1114.
2. Scheer, H. In *Chlorophylls and Bacteriochlorophylls: Biochemistry, Biophysics, Functions and Applications*; Grimm, B., Porra, R. J., Rüdiger, W., Scheer, H., Eds.; Springer: Dordrecht, 2006; pp 1–26.
3. Melkozernov, A. N.; Blankenship, R. E. In *Chlorophylls and Bacteriochlorophylls: Biochemistry, Biophysics, Functions and Applications*; Grimm, B., Porra, R. J., Rüdiger, W., Scheer, H., Eds.; Springer: Dordrecht, 2006; pp 397–412.
4. Porra, R. J. *Photochem. Photobiol.* **1997**, *65*, 492.
5. Frigaard, N.-U.; Chew, A. G. M.; Maresca, J. A.; Bryant, D. A. In *Chlorophylls and Bacteriochlorophylls: Biochemistry, Biophysics, Functions and Applications*; Grimm, B., Porra, R. J., Rüdiger, W., Scheer, H., Eds.; Springer: Dordrecht, 2006; pp 201–221.
6. Tanaka, R.; Tanaka, A. *Annu. Rev. Plant Biol.* **2007**, *58*, 321.
7. Masuda, T.; Fujita, Y. *Photochem. Photobiol. Sci.* **2008**, *7*, 1131.
8. Chew, A. G. M.; Bryant, D. A. *Annu. Rev. Microbiol.* **2007**, *61*, 113.
9. Tamiaki, H.; Shibata, R.; Mizoguchi, T. *Photochem. Photobiol.* **2007**, *83*, 152.
10. Tamiaki, H.; Kunieda, M. In *Handbook of Porphyrin Science*; Kadish, K. M., Smith, K. M., Guilard, R., Eds.; World Scientific: Singapore, 2010; Vol. 11, pp 223–289. Chapter 51.
11. Chen, M.; Schliep, M.; Willows, R. D.; Cai, Z.-L.; Neilan, B. A.; Scheer, H. *Science* **2010**, *329*, 1318.
12. Harada, J.; Mizoguchi, T.; Tsukatani, Y.; Noguchi, M.; Tamiaki, H. *Sci. Rep.* **2012**, *2*. doi: http://dx.doi.org/10.1038/srep00671.
13. Vogl, K.; Tank, M.; Orf, G. S.; Blankenship, R. E.; Bryant, D. A. *Front. Microbiol.* **2012**, *3*. doi: http://dx.doi.org/10.3389/fmicb.2012.00298.
14. Reinbothe, C.; Bakkouri, M. El.; Buhr, F.; Muraki, N.; Nomata, J.; Kurisu, G.; Fujita, Y.; Reinbothe, S. *Trends Plant Sci.* **2010**, *15*, 614.
15. Muraki, N.; Nomata, J.; Ebata, K.; Mizoguchi, T.; Shiba, T.; Tamiaki, H.; Kurisu, G.; Fujita, Y. *Nature* **2010**, *465*, 110.
16. Nagata, N.; Tanaka, R.; Satoh, S.; Tanaka, A. *Plant Cell* **2005**, *17*, 233.
17. Nakanishi, H.; Nozue, H.; Suzuki, K.; Kaneko, Y.; Taguchi, G.; Hayashida, N. *Plant Cell Physiol.* **2005**, *46*, 467.
18. Olson, J. M. *Photochem. Photobiol.* **1998**, *67*, 61.
19. Kobayashi, M.; Oh-oka, H.; Akutsu, S.; Akiyama, M.; Tominaga, K.; Kise, H.; Nishida, F.; Watanabe, T.; Amesz, J.; Koizumi, M.; Ishida, N.; Kano, H. *Photosynth. Res.* **2000**, *63*, 269.
20. Eisen, J. A.; Nelson, K. E.; Paulsen, I. T.; Heidelberg, J. F.; Wu, M.; Dodson, R. J.; Deboy, R.; Gwinn, M. L.; Nelson, W. C.; Haft, D. H.; Hickey, E. K.; Peterson, J. D.; Durkin, A. S.; Kolonay, J. L.; Yang, F.; Holt, I.; Umayam, L. A.; Mason, T.; Brenner, M.; Shea, T. P.; Parksey, D.; Nierman, W. C.; Feldblyum, T. V.; Hansen, C. L.; Craven, M. B.; Radune, D.; Vamathevan, J.; Khouri, H.; White, O.; Gruber, T. M.; Ketchum, K. A.; Venter, J. C.; Tettelin, H.; Bryant, D. A.; Fraser, C. M. *Proc. Natl. Acad. Sci. U.S.A.* **2002**, *99*, 9509.
21. Suzuki, J. Y.; Bauer, C. E. *J. Biol. Chem.* **1995**, *270*, 3732.
22. Chew, A. G. M.; Bryant, D. A. *J. Biol. Chem.* **2007**, *282*, 2967.

23. Blankenship, R. E.; Matsuura, K. In *Light-Harvesting Antennas in Photosynthesis*; Green, B. R., Parson, W. W., Eds.; Kluwer Academic Publishers: Dordrecht, 2003; pp 195–217.
24. Balaban, T. S.; Tamiaki, H.; Holzwarth, A. R. *Top. Curr. Chem.* **2005**, *258*, 1.
25. Miyatake, T.; Tamiaki, H. *J. Photochem. Photobiol., C* **2005**, *6*, 89.
26. Iwaki, M.; Itoh, S.; Kamei, S.; Matsubara, H.; Oh-oka, H. *Plant Cell Physiol.* **1999**, *40*, 1021.
27. Chew, A. G. M.; Frigaard, N.-U.; Bryant, D. A. *J. Bacteriol.* **2007**, *189*, 6176.
28. Balaban, T. S.; Holzwarth, A. R.; Schaffner, K.; Böender, G.-J.; de Groot, H. J. M. *Biochemistry* **1995**, *34*, 15259.
29. Mizoguchi, T.; Hara, K.; Nagae, H.; Koyama, Y. *Photochem. Photobiol.* **2000**, *71*, 596.
30. Goericke, R.; Repeta, D. J. *Limnol. Oceanogr.* **1992**, *37*, 425.
31. Tamiaki, H.; Takekoshi, D.; Mizoguchi, T. *Bioorg. Med. Chem.* **2011**, *19*, 52.
32. Wahlund, T. M.; Madigan, M. T. *J. Bacteriol.* **1995**, *177*, 2583.
33. Frigaard, N.-U.; Bryant, D. A. *Appl. Environ. Microbiol.* **2001**, *67*, 2538.
34. Schweizer, H. D. *BioTechniques* **1993**, *15*, 831.
35. Harada, J.; Miyago, S.; Mizoguchi, T.; Azai, C.; Inoue, K.; Tamiaki, H.; Oh-Oka, H. *Photochem. Photobiol. Sci.* **2008**, *7*, 1179.